

LA-UR-18-22995

Approved for public release; distribution is unlimited.

Title: Progress Towards an Indirect Neutron Capture Capability at LANSCE:
October 2017 – March 2018

Author(s): Koehler, Paul E.
Ullmann, John Leonard
Couture, Aaron Joseph
Mosby, Shea Morgan

Intended for: Report

Issued: 2018-04-09

Disclaimer:

Los Alamos National Laboratory, an affirmative action/equal opportunity employer, is operated by the Los Alamos National Security, LLC for the National Nuclear Security Administration of the U.S. Department of Energy under contract DE-AC52-06NA25396. By approving this article, the publisher recognizes that the U.S. Government retains nonexclusive, royalty-free license to publish or reproduce the published form of this contribution, or to allow others to do so, for U.S. Government purposes. Los Alamos National Laboratory requests that the publisher identify this article as work performed under the auspices of the U.S. Department of Energy. Los Alamos National Laboratory strongly supports academic freedom and a researcher's right to publish; as an institution, however, the Laboratory does not endorse the viewpoint of a publication or guarantee its technical correctness.

Progress Towards an Indirect Neutron Capture Capability at LANSCE: October 2017 – March 2018

P. E. Koehler, J. L. Ullmann, A. Couture, and S. Mosby

P-27, Los Alamos National Laboratory

Abstract: We describe progress developing the Device for Indirect Capture Experiments on Radionuclides (DICER) on flight path 13 at the Lujan Center at the Los Alamos Neutron Science Center (LANSCE). This capability is being developed to tightly constrain neutron-capture cross section on short-lived radioactive nuclides of high importance to weapons-program sponsors via neutron total cross section measurements on the same nuclides. In this report, we describe progress in this endeavor during October 2017 through March 2018.

I. Introduction

During this period, the following progress was made. 1) Measurements were made with several samples to assess the effect of improvements to DICER made during the previous FY. 2) Most of the remaining section of neutron guide outside the bulk shield was replaced by a vacuum pipe containing two new sets of collimators. 3) A highly enriched ^{95}Mo sample was purchased and first test measurements were made with this sample. 4) A new tool was developed to quickly calculate theoretical neutron-capture cross sections for a wide range of nuclear-level-density and photon-strength-function models and compare the results to cross sections in use at LANL. 4) More analysis of DICER and other data on ^{197}Au revealed a sensitivity to the nuclear spin distribution at high excitation. 5) An LDRD pre-proposal for DICER was developed and submitted. 6) A talk on DICER was presented at the 9th Tri-Lab (JOWOG) Nuclear Data Workshop. More information on each of these topics is given below.

II. Measurements to assess effect of DICER beam-line improvement from last FY

The main improvement to the DICER beam line during FY17 [1] was to replace the massive shielding “cave” near the detector with a low-mass “Morgan” building. This change was expected to reduce background due to neutrons scattered from the detector which subsequently rebound from the cave walls back into the detector at later times. Although fairly small, this background is sample dependent and has been shown to be impossible to measure or to accurately simulate at other facilities. Measurements before and after the change made with samples (^{169}Tm , ^{209}Bi , $^{\text{nat}}\text{Cu}$) having black resonances indicate this background has been reduced as expected.

III. New beam pipe and collimation

Most of the old neutron guide in the region between the shutter (7 m from the source) and the sample (30 m from the source) has been replaced by a 10” diameter vacuum pipe containing two new sets of collimators. In addition, this new beam pipe was designed so that both the sample and detector positions could be moved to shorter flight paths with minimal work, enabling more measurement flexibility. The neutron guide was part of the old materials science instrument on flight path 13. Above thermal energy, this guide scattered neutrons along its entire length thereby increasing the background level in DICER. In addition, the beam at the sample collimator was very large and poorly defined, resulting in more scattered

background further downstream closer to the detector position. In contrast, the new arrangement limits the scattering to the two collimator locations, which can be shielded much more effectively, and results in a smaller, well-defined beam at the sample collimator. Beam images taken just before the sample position before this change was made revealed that the beam was seriously off center and differed substantially from the expected circular shape. While the new beam pipe and collimators were being installed, it was discovered that the last remaining section of guide outside the bulk shield (which has been deemed too difficult to remove, at present) was seriously misaligned. Considerable effort was made to realign the entire beam line, secure this guide section so that it remains aligned, and installing new alignment targets so that future alignments will be easier.

Fig. 1 shows the end result of these efforts. The beam spot at the sample position is now much closer to expectations. Unfortunately, these changes took almost the entire run cycle to complete and so not enough time was left to fully measure their effect. The next section describes the first measurements made after these improvements.

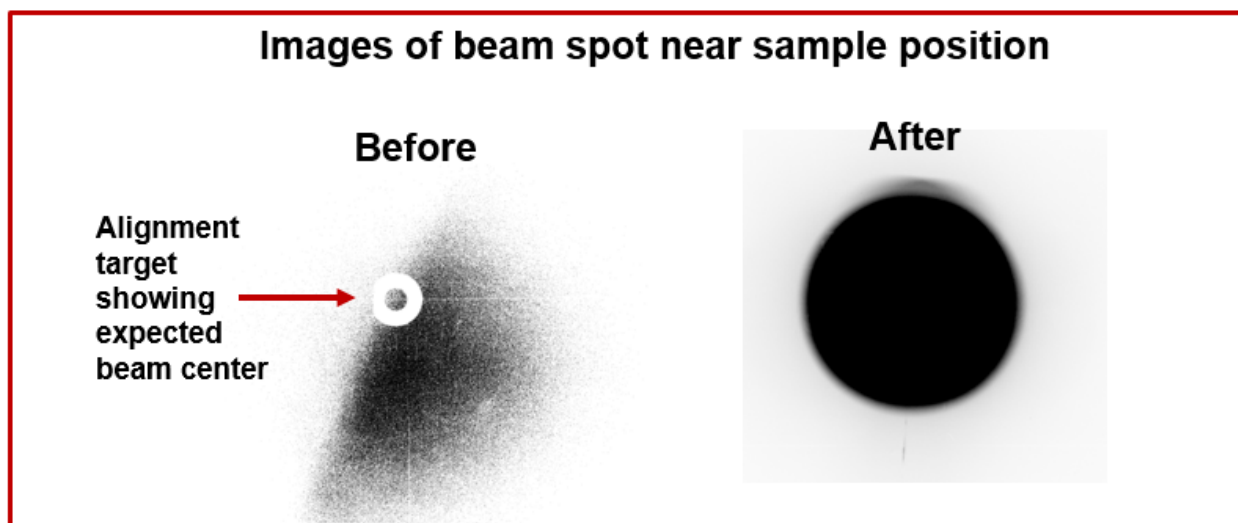


Figure 1. Beam images before (left) and after (right) installing new beam pipe and collimators between the shutter and sample, and realigning the last remaining section of neutron guide outside the bulk shield. The beam is expected to be centered and circular at this position. The poorly aligned neutron-guide section resulted in a misaligned and misshapen beam spot in the “before” image. After realignment and installation of the new collimators, the beam image is much closer to expectations.

IV. Measurements with a highly enriched ^{95}Mo sample

A molybdenum sample enriched to 96.79% in ^{95}Mo was purchased from ORNL isotopes. ^{95}Mo was chosen as a test bed for future ^{88}Y measurement because theory predicts the latter should have an average resonance spacing ($D_0 \approx 20 - 200$ eV) close to that measured ($D_0 = 66.1 \pm 3.0$ eV) for the former, and because excellent $^{95}\text{Mo}+n$ resonance parameters exist [2]. To facilitate comparison to these previous data, the same sample thickness was ordered. To minimize cost, a diameter (7.0 mm) slightly larger than our current 6-mm-diameter collimator was chosen. The plan is to make transmission measurements with various collimator sizes and flight-path lengths to assess ^{88}Y measurement feasibility.

Unfortunately, by the time the beam line improvements described above were completed, only a few weeks of beam time remained in the run cycle. After shakedown and calibration of the apparatus, only enough time was left for a measurement with this sample using the 6-mm-diameter collimator with the

sample at 30 m and the detector at 64 m. These data are being analyzed. The plan is to continue these measurements next run cycle. We also had planned to do similar measurements with a highly enriched ^{195}Pt sample as a test bed for radionuclides having smaller resonance spacings (e.g. $^{167,168,170,171}\text{Tm}$). However, at present we do not have the resources to purchase this sample.

V. Development of a new software tool for calculating the range of theoretical neutron-capture cross sections and comparing them to the current LANL dosimetry library

The nuclear statistical model (NSM) code talys [3] is used by researches worldwide to predict cross sections for nuclides beyond the reach of measurement. This code contains six nuclear level density (NLD) and eight photon-strength-function (PSF) models which can be used in cross-section predictions. Although these models have been tuned to produce similar results for stable nuclides where data exist, predictions for unmeasured radionuclides can vary by sizeable factors. As written, a talys calculation for each NLD-PSF combination requires its own input file and produces its own set of output files. Therefore, assessing the range of calculations for all 48 NLD-PSF combinations requires running as many calculations and piecing together as many outputs. Hence, a program was written to automatically run through the 48 possible combinations, piece together the outputs into a single file, and construct the minimum and maximum cross-section range as a function of energy suitable for plotting. This greatly reduces the time needed to generate the range of talys predictions and compare them to values currently in use at LANL.

Figs. 2 and 3 show results for ^{88}Y and ^{168}Tm produced with this new tool. In the case of ^{88}Y , talys predictions span as much as a factor of 20, indicating that this cross section is more uncertain than typical for a nuclide only one mass unit from stability. However, this is not too surprising because ^{88}Y is only one neutron shy of a closed shell and hence in a region where the average resonance spacing varies rapidly as a function of mass, and therefore very difficult to predict with any accuracy. Interestingly, the LANL value has steadily increased over the years to where it currently is near the middle of the range predicted by talys. In addition to a wide magnitude range, the talys predictions also have a wide range of shapes. As the shape of the LANL value is even more poorly constrained than its magnitude, the wide range of shapes predicted by talys is troubling.

Fig. 2 also includes the $^{88}\text{Y}(n,\gamma)$ cross section suggested by recent data [4] obtained with the Oslo technique. This method measures a product of quantities related to the NLD and PSF and requires some assumptions as well as calibrations to predict cross sections. The most important calibrations require knowledge of the average resonance spacing D_0 and the average total capture width $\langle\Gamma_{\gamma 0}\rangle$ at the neutron threshold. Because these quantities have not been measured, the Oslo data are essentially normalized using theory. Specifically, they chose an average *s*-wave resonance spacing ($D_0 \approx 130$ eV) about 10 times larger than used to obtain the current LANL cross section [5]. Because the neutron-capture cross section is inversely proportional to D_0 , the Oslo cross section is much smaller than the LANL value. When DICER is operational, we will be able to measure both D_0 and $\langle\Gamma_{\gamma 0}\rangle$ and hence leverage the Oslo data to obtain an even more tightly constrained $^{88}\text{Y}(n,\gamma)$ cross section.

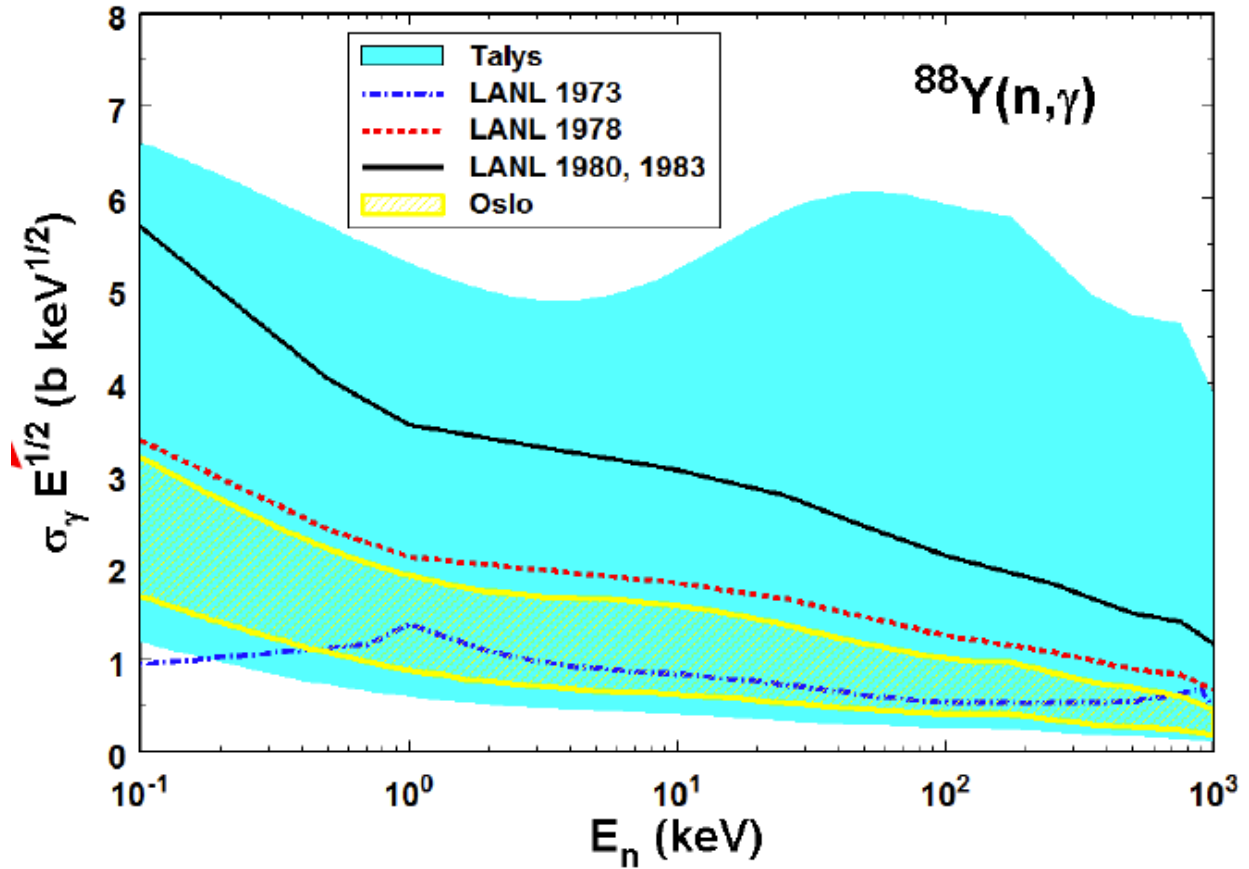


Figure 2. Range of $^{88}\text{Y}(n,\gamma)$ cross section predicted by talys (cyan area) compared to values from the 1973 (blue dot dashed curve), 1978 (red dashed curve), and current [5] (black solid curve) LANL libraries. Also shown (yellow cross-hatched area) is the value estimated for this cross section from Ref. [4].

The range of $^{168}\text{Tm}(n,\gamma)$ cross sections predicted by the 48 combinations of NLD and PSF models available in talys is compared to LANL library values in Fig. 3. In this case, the range of talys predictions is a bit smaller. However, it is disconcerting that the current LANL cross section is mostly outside the range predicted by talys, whereas the previous 1997 LANL value [6] is close to the middle of the range predicted by talys. Some details of the impact of these difference on radiochemical diagnostics can be found in Ref. [7]. Tightly constraining this cross section should be possible when DICER is operational.

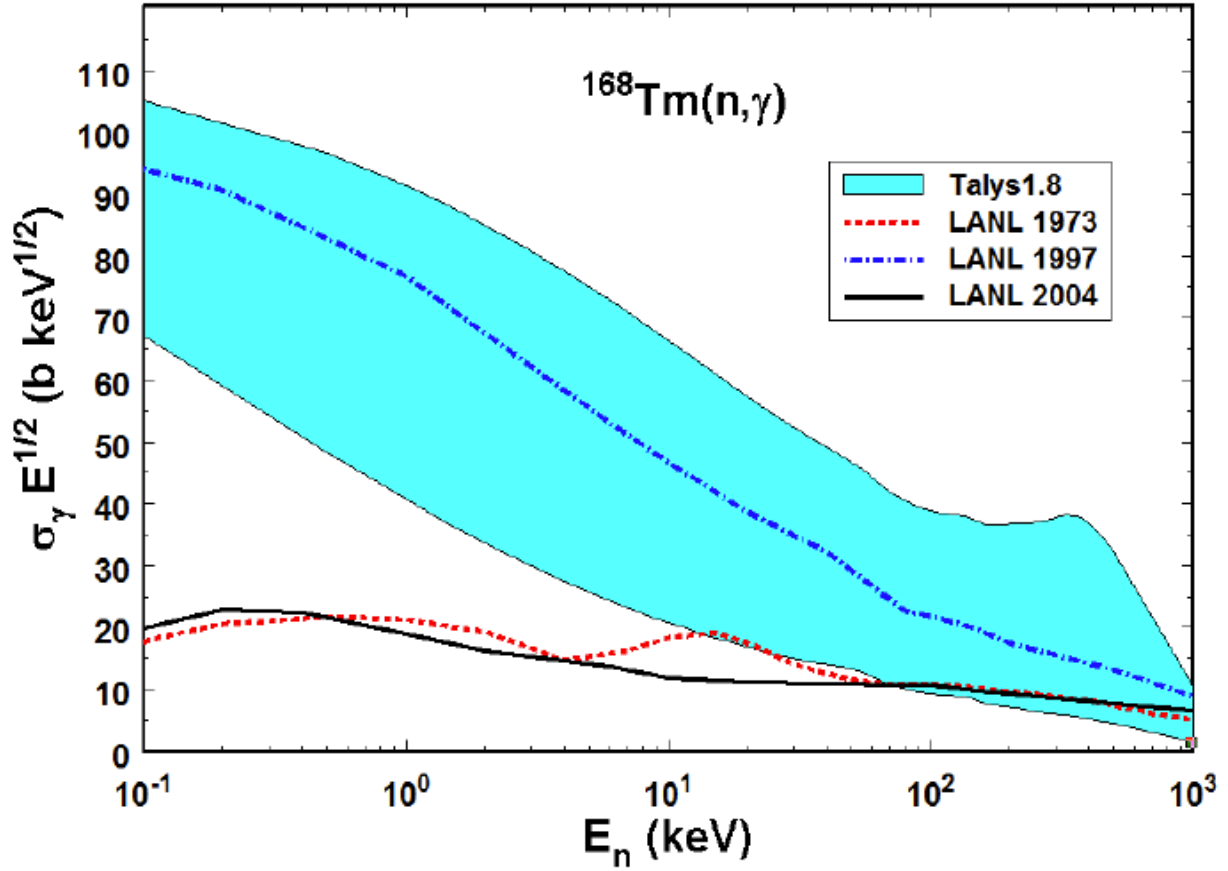


Figure 3. Range of $^{168}\text{Tm}(n,\gamma)$ cross sections predicted by talys (cyan area) compared to the current (solid black curve) and previous (dot-dashed blue and dashed red curves) LANL libraries.

VI. Using DICER data to constrain the nuclear spin distribution at high excitation

In previous reports, we have describe how the Γ_γ distribution data (blue circles and red X's for J=1 and 2 resonances, respectively) in Fig. 4 were obtained from a simultaneous *R*-matrix fit to data from DICER, *n*_TOF [8], and GELINA [9], and that the data disagree with NSM simulations (blue and red dashed curves for J=1 and 2, respectively) using the NLD and PSF measured with the Oslo technique [10]. In addition to normalizations to D_0 and $\langle\Gamma_{\gamma 0}\rangle$ as described above, the Oslo technique requires the spin distribution as a function of excitation energy. For most intermediate- to heavy-mass nuclides, this distribution is very poorly, if at all, constrained by data except close to the ground state. Hence, this quantity typically is obtained from a nuclear model.

The spin distribution affects the simulated Γ_γ distributions in two ways. First, the relative sizes of the average Γ_γ values for J=1 and 2 depends on the relative number of J=0 to J=3 levels. To see how this is the case, it's important to know that the measured total gamma width for each resonance Γ_γ is equal to the sum of all the partial gamma widths $\Gamma_{\gamma i}$ for (primary) decay from the resonance to levels at lower excitation; $\Gamma_\gamma = \sum \Gamma_{\gamma i}$. In addition, dipole decay dominates so J=1 resonances can decay to J=0, 1, and 2 whereas J=2 resonances can decay to J=1, 2, and 3. Therefore, since both spins can decay to J=1 and 2, the relative sizes of the average Γ_γ values for J=1 and 2 depends on the relative number

of $J=0$ to $J=3$ levels. Second, the assumed spin distribution affects the resultant slope of the PSF and a steeper PSF results in broader Γ_γ distributions and vice versa.

Simulations with a modified spin distribution are shown as solid blue and red curves for $J=1$ and 2 , respectively, in Fig. 4. These simulations are in much better agreement with the data than simulations using the spin distribution assumed by the Oslo group.

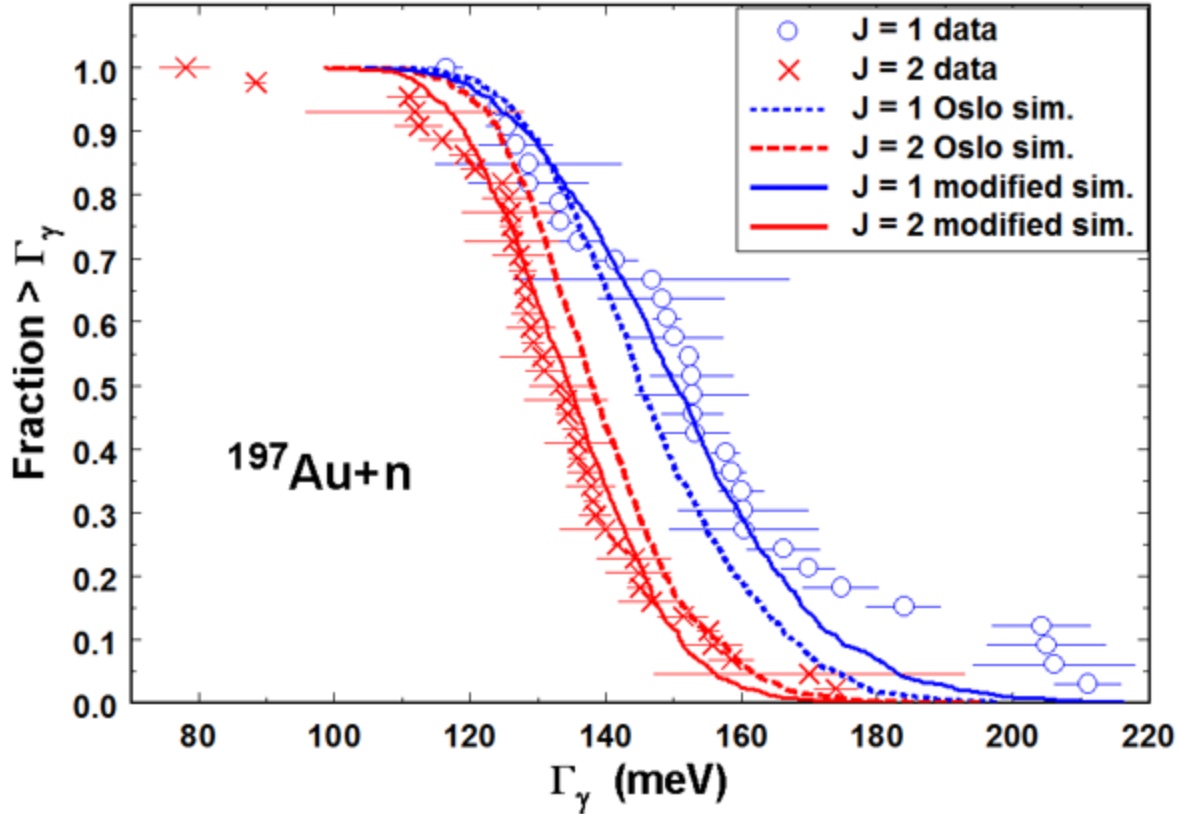


Figure 4. Total gamma width distributions for $J=1$ (blue circles) and $J=2$ (red X's) for $^{197}\text{Au}+n$ resonances obtained from simultaneous R-matrix analysis of data from DICER, n_TOF [8], and GELINA [9]. Also shown are NSM simulations of the expected distributions (dashed curves) using reported NLD and PSF results [10] from the Oslo technique. Solid curves depict simulations employing a modified spin distribution. See text for more details.

This is another example of how DICER data can improve nuclear models and leverage data obtained at other facilities to better constrain neutron-capture cross sections of importance to the weapons programs. This may become increasingly important when FRIB comes on line and researchers attempt to use the β -Oslo technique to obtain NLD's and PSF's for constraining neutron-capture cross sections for radionuclides. At present, β -Oslo data are normalized using theory, but DICER measurements, to obtain D_0 and $\langle \Gamma_{\gamma 0} \rangle$ on the same nuclides, would put β -Oslo results on much firmer footing by basing these normalizations on data.

VII. DICER LDRD pre-proposal submitted

An LDRD DR proposal [11] entitled "Putting the Gold Standard for LANL's Dosimetry Network on a Firm Basis" was submitted. The proposal team members are Paul Koehler (PI, P-27), Aaron Couture (P-

27), Morgan White (XCP-5), John Ullmann (P-27), Francois Nortier (C-IIAC), August Keksis (C-NR), Todd Bredeweg (C-NR), and Gencho Rusev (C-NR). The abstract for this proposal is reproduced in the next paragraph.

Radiochemical diagnostics have been a crucial ingredient of nuclear weapons testing since its inception, and efforts continue to this day to increase their usefulness and predictive capability. We will put yttrium, the gold standard for LANL's dosimetry network, on a firm experiment basis by tightly constraining the $^{88}\text{Y}(n,\gamma)$ cross section via a novel, proven technique. Best theory estimates of this cross sections vary by factors of 5 – 30 over the region of interest. Our innovative method takes advantage of the world-leading neutron flux and resolution at the Lujan Center and radioisotope production capabilities at the Isotope Production Facility, and LANL's expertise in radiochemistry, neutron-resonance measurements, and nuclear evaluations to constrain this important cross section to ~10%. Our proposal directly addresses priority 1 of Nuclear and Particle Futures; "...understanding of the behavior of nuclear interactions (and the role hydrodynamics plays in driving these interaction) in extreme environments: astrophysical systems, weapons environments, and/or dense nuclear matter." If successful, our research will eliminate a key source of uncertainty in the gold standard of LANL's dosimetry network. Furthermore, the techniques developed are directly applicable to future measurements of high importance to this field as well as the closely-related area of nuclear forensics.

VIII. DICER talk presented at workshop

Paul Koehler presented a talk on DICER at the 9th Tri-Lab (JOWOG) Nuclear Data Workshop [12]. In addition to describing the technique and current status, improvements to DICER and other nuclear physics experiments at the Lujan Center enabled by the new neutron production target [13] (expected to be installed in 2020), and leveraging data from other facilities using DICER data also were discussed.

References

- [1] P. E. Koehler, J. L. Ullmann, A. J. Couture, and S. M. Mosby, "Progress Towards an Indirect Neutron Capture Capability at LANSCE", LA-Ur-17-28521.
- [2] P. E. Koehler, A. C. Larsen, M. Guttormsen, S. Siem, and K. H. Guber, "Extreme Nonstatistical Effects in γ Decay of ^{95}Mo Neutron Resonances", *Phys. Rev. C* **88**, 041305(R) (2013).
- [3] A. J. Koning, S. Hilaire, and M. C. Duijvestijn, in *Proceedings of the International Conference on Nuclear Data for Science and Technology - ND2007*, edited by O. Bersillon *et al.* (EDP Sciences, Les Ulis, France, 2008), p. 211.
- [4] A. C. Larsen *et al.*, "Experimentally Constrained $(p,\gamma)^{89}\text{Y}$ and $(n,\gamma)^{89}\text{Y}$ Reaction Rates Relevant to p -process Nucleosynthesis", *Phys. Rev. C* **93**, 045810 (2016).
- [5] M. B. Chadwick *et al.*, "Evaluated Iridium, Yttrium, and Thulium Cross Sections and Integral Validation Against Critical Assembly and Bethe Sphere Measurements", *Nuclear Data Sheets* **108**, 2716 (2007).
- [6] P. G. Young and L. Liu, "Analysis of $n + ^{169}\text{Tm}$ Reactions from 0.1 keV to 30 MeV and prediction of $^{168}\text{Tm}(n,2n)$ and $^{171}\text{Tm}(n,\gamma)$ Cross Sections," LA-UR 97-4900.
- [7] S. Becker, "Comparison of Bigmac Calculations (2-9-05), X-2: 05: 009.
- [8] C. Massimi *et al.*, " $^{197}\text{Au}(n,\gamma)$ Cross Section in the Resonance Region", *Phys. Rev. C* **81**, 044616 (2010).
- [9] I. Sirakov *et al.*, "Results of Total Cross Section Measurements for ^{197}Au in the Neutron Energy Region from 4 to 108 keV at GELINA", *Eur. Phys. J. A* **49**, 144 (2013).
- [10] F. Giacoppo *et al.*, " γ Decay from the Quasicontinuum of $^{197,198}\text{Au}$ ", *Phys. Rev. C* **91**, 054327 (2015).
- [11] LDRD pre-proposal 20190150DR.
- [12] P. E. Koehler, "Tightly Constraining Neutron-Capture Cross Sections for Nuclear Forensics and Radiochemical Diagnostics via Total-Cross-Section Measurements at LANSCE", LA-UR-18-21567.
- [13] P. E. Koehler *et al.*, "Proposed Science Design for the Mark-IV 1L Target", LA-UR-17-29834.